Technical and energetic assessment of a three-stage thermochemical treatment for sewage sludge

Javier Ábrego[a]*, *José Luis Sánchez*[a], *Jesús Arauzo*[a], *Isabel Fonts*[a,b], *Noemí Gil-Lalaguna*[a], *María Atienza-Martínez*[a]

[a] Aragón Institute of Engineering Research (I3A), University of Zaragoza, c/ Mariano Esquillor s.n., 50018, Zaragoza, Spain.

[b] Centro Universitario de la Defensa, Ctra. Huesca s/n, 50090 Zaragoza, Spain.

*javabr@unizar.es.

A three-stage thermochemical process comprising torrefaction, pyrolysis and char activation is proposed for the treatment of dry sewage sludge or biomass materials. To assess the feasibility of the process, lab-scale experiments were carried out with dried sewage sludge as feedstock, and mass and energy balances were calculated. In the process, 19.3 % of the sewage sludge initial weight was transformed into a bio-oil with three distinct phases and reduced water content (66.1% of water content in the aqueous phase compared to 73.8 % in a single-step fast pyrolysis). The product gases had a high H_2S content but also enough heating value to be combusted. After being activated by the torrefaction vapors, the solid fraction (48.2 % of the initial sludge weight) showed certain pore development and might be suitable for adsorption applications. Regarding the energy balance, it was found that combustion of part of the product gas would provide the necessary heat to drive the process (1019 kJ/kg of dry sewage sludge).

KEYWORDS Thermochemical process, pyrolysis, torrefaction, adsorbent, sewage sludge.

1. INTRODUCTION

Several types of thermochemical treatments for biomass have gained much interest in the last few years. Among them, pyrolysis is one of the most promising. Although there are still important issues to overcome, some of these processes have reached commercial or semi-commercial status. This is not the case for sewage sludge, due to its differences with lignocellulosic biomass. Reduced heating value and high ash, nitrogen and sulfur content are the main factors limiting the use of this material in thermochemical processes.

There are scarce recent references of thermochemical treatments for sewage sludge at pilot-scale size. The *Enersludge* process was developed in Australia, and some operational results have been reported[1,2]. Additionally, a patented flash carbonization process has been used at the University of Hawai'i for various feedstock, including sewage sludge for *Terra Preta* applications[3]. A greater number of studies can be found for laboratory small-scale studies. For instance, sewage sludge pyrolysis for liquid production has been the subject of several works in the last few years[4]. Fluidized bed reactors are predominantly used because high heating rates and a good temperature control can easily be achieved[5]. It is well known that a high selectivity to the liquid fraction is found at intermediate temperatures. Thus, Kim and Parker[6] determined an optimal temperature of 500ºC for maximum liquid production, whereas Shen and Zhang[7] and Fonts et al.[8] reported slightly higher values (525 and 540ºC respectively). Some of the most important issues for bio-oil quality are its instability and difficulty to blend with other fuels[9], usually attributed to oxygen content, and its relatively low heating value and separation of phases, related to its water content[10].

Another lab-scale approach for sewage sludge valorization has been adsorbent production. A review paper recently summarized the work carried out on this subject[11]. Usually, chemical activation stages using alkali metal hydroxides are most effective towards high surface area adsorbents. Without chemical

activation, single-step pyrolysis of sewage sludge produces chars with low surface areas. Surface area can be slightly increased by physical activation, by means of an additional burn-off of the solid by air, CO_2 or H_2O. Thus, many works in the last decades have dealt with pyrolysis of sewage sludge for fuel or chemicals, but research has been mostly focused on only one product fraction (liquid or solid) without performing a global study of the process products, or combining different treatments.

A process that has recently been the focus of remarkable interest is torrefaction[12]. This process has been proposed primarily as a treatment prior to gasification[13,14] or combustion of biomass resources, but to the best of our knowledge has rarely been associated with a pyrolysis treatment afterwards[15,16]. Only recently, a research paper has discussed in detail the combination of torrefaction and pyrolysis[17]. It is known that torrefaction produces CO_2 and H_2O as major gaseous and liquid compounds, respectively[18]. A mixture of condensable organic liquids is also formed, and its distribution is strongly dependent on the initial biomass composition and process conditions[19]. A preliminary stage of sewage sludge torrefaction could help to improve the final characteristics of the liquid yield from pyrolysis, lowering its water content (due to previous release of this compound) and thus improving its heating value.

With the aim of studying the integral valorization of sewage sludge, we propose a novel process for sewage sludge that combines several thermochemical treatments (torrefaction, pyrolysis and char activation) to yield valuable solid, liquid and gaseous fractions simultaneously. Furthermore, this approach could be extended for similar residues and/or lignocellulosic biomass.

A simplified overview of the process can be seen in Figure 1. As a result of the torrefaction step (carried out prior to pyrolysis), a reduction of the water content of bio-oil from pyrolysis is expected. This reduction would have a direct impact in the heating value of bio-oil and could also be beneficial to its physicochemical properties[10]. Additionally, the pyrolysis gas would have higher heating value as a result of the previous removal of a significant fraction of CO_2. Water and CO_2 from torrefaction can be used as activation agents for the char product obtained in the pyrolysis step. In this way, additional

combustible gases and an adsorbent are produced. The latter might be suitable for desulfurization processes, as shown by previous works[20,21].

The technical and energetic feasibility of the process was assessed by means of lab-scale experiments and mass and energy balances.

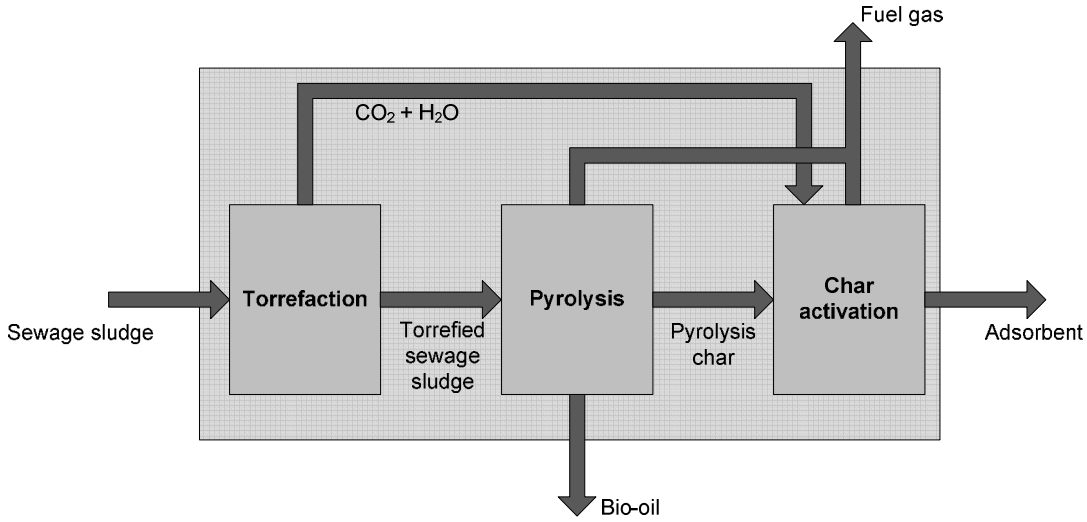

Figure 1. Schematic diagram of the proposed process.

2. EXPERIMENTAL

The three proposed stages were carried out separately in laboratory scale facilities using sewage sludge as raw material. All the experiments were duplicated. Anaerobically digested and thermally dried sludge was supplied by an urban wastewater treatment plant located in Madrid, Spain. Proximate and ultimate analyses of this sludge and its solid and liquid products were performed at the Instituto de Carboquímica (ICB-CSIC) in Zaragoza, Spain. Analysis of raw sewage sludge is shown in Table 1. Heating value of the sewage sludge and the liquid phases obtained from pyrolysis was determined using a C2000 IKA calorimeter.

Table 1. Ultimate/proximate analyses and heating value of sewage sludge.

	% weight	
Proximate Analysis	Dry basis	As received
Moisture (ISO-589-1981)	-	8.9
Ash (ISO-1171-1976)	46.3	42.1
Volatiles (ISO-5623-1974)	46.44	42.3
Fixed Carbon (by diff.)	7.3	6.7
Ultimate analysis (Carlo Erba 1108)		
C	29.7	27.1
H	3.6	4.3
N	4.4	4.0
S	0.9	0.9
O (by difference)	15.0	21.6
Heating Value	(MJ/kg)	
HHV	11.4	
LHV	10.3	

2.1. TORREFACTION EXPERIMENTS

In order to evaluate the optimal conditions for the torrefaction stage, preliminary experiments were performed at a laboratory-scale fixed bed pyrolysis plant, described elsewhere[20]. For each experiment, 3.0 g of sewage sludge were placed inside the reactor. Three final temperatures were tested: 250, 300 and 350ºC. A heating rate of 10 ºC/min was applied, and an additional hold time of 30 minutes was maintained after reaching the desired final temperature. During the experiments, an inert atmosphere was maintained by flowing 100 ml (STP)/min of N_2 (STP: 0°C and 1 atm) through the reactor vessel.

After the experiments, the solid and liquid fractions were determined gravimetrically. The gaseous fraction was calculated by difference, and its composition (as well as all the gaseous compositions in

this work) was determined by means of an Agilent 3000A MicroGC portable chromatograph. Additionally, the water content of the liquid fraction was determined by Karl-Fischer titration.

2.2. PYROLYSIS EXPERIMENTS

Torrefied sewage sludge was then pyrolyzed in a lab-scale fluidized bed facility, as described previously[8,22]. Torrefied sewage sludge was continuously introduced into the fluidized bed by means of a screw feeder with a feeding rate of 3.0 g/min. Nitrogen was the inert gas with a total flow of 4.5 l (STP)/min. Two-thirds of this flow was introduced directly into the reactor, while the rest was introduced through the screw feeder to aid homogeneous solid feedstock delivery. After a cyclone and a hot gas filter (450ºC), pyrolysis vapors were cooled down in a series of systems consisting of two condensers and an electrostatic precipitator. The collected liquid (bio-oil) was weighted and analyzed to determine its ultimate analysis and its water content. Non-condensable gases were measured by a volumetric gas meter and its composition was determined by chromatography.

The described pyrolysis plant is much larger than the previously described fixed bed torrefaction facility; thus, a great number of identical experiments would have been necessary in order to obtain a sufficient amount of torrefied sewage sludge to be used in the fluidized bed. For this reason, additional torrefaction experiments were done in this plant at the optimum torrefaction temperature, which was previously determined. The total time for these experiments was 1 hour.

2.3. EXPERIMENTS FOR ACTIVATION OF PYROLYSIS CHAR

For each activation experiment, 3.0 g of char from pyrolysis were introduced in the same fixed bed plant previously described. Two activation temperatures were tested: 750 and 850ºC. Each experiment was divided into two stages; in the first one, char was heated up to the desired activation temperature. Because this activation temperature was higher than any of those previously applied, char was further pyrolyzed while being heated; thus, additional combustible gases were generated. After reaching the final temperature, the activating agents were introduced. A mass flow controller gave the desired flow

rate of CO_2, which was mixed with nitrogen. The desired flow of water vapor was achieved by bubbling these gases through a water vessel that was heated to reach the required vapor pressure. The total gas flow was 100 ml (STP)/min of gases. Activating agents were fed for one hour, and the total amount of CO_2 + H_2O fed during that time was equal to the measured amount of these two products in the torrefaction experiment at the optimum temperature. Gas composition was determined throughout all the experiments, and the final solid product was weighed and analyzed (BET surface area and elemental analysis). A refrigerated condenser and a cotton filter were used to collect the liquid products, which were also weighed.

3. RESULTS AND DISCUSSION

3.1. TORREFACTION STAGE

3.1.1. FIXED BED TORREFACTION EXPERIMENTS

The product distribution (solid, liquid and gaseous yields) obtained from the torrefaction experiments are shown in Table 2. As expected, an increase in torrefaction temperature causes a decrease in the solid yield and subsequent increases in liquid and gas yields. Liquid products account for a significant part of the solid weight loss (up to more than 25% at the highest temperature). Nevertheless, and due to the high ash content of sewage sludge, the observed solid yields are relatively high (64.3%) even after torrefaction at 350ºC.

Table 2. Product distribution of fixed bed torrefaction experiments.

Temperature (ºC)	Weight % of each fraction (on sludge basis)		
	Solid	Liquid	Gas
250	81.9 ± 0.3	15.3 ± 0.4	2.9 ± 0.0
300	71.7 ± 0.0	19.9 ± 1.3	8.4 ± 1.2
350	64.3 ± 0.3	26.5 ± 0.9	9.3 ± 0.9

The higher heating values of torrefied sewage sludge are shown in Figure 2. At the highest temperatures within this interval, there is a significant decrease in the heating value of solids.

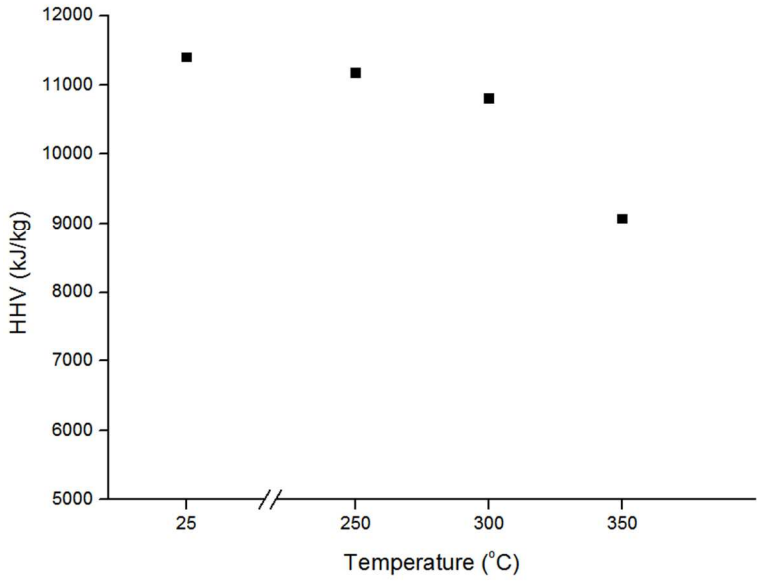

Figure 2. Higher Heating Values (kJ/kg) of torrefied sewage sludge (fixed bed torrefaction).

Combining this data with solid yields from Table 2, the energy content of the solids (based on the initial energy content of sludge) can be calculated. For instance, torrefaction at 350 ºC produces a solid that contains only around 51.2% of the original energy from sludge, whereas the energy loss is not as high for lower temperatures (32 and 19.8% for 300 and 250ºC, respectively). According to these data, 350ºC seems to cause an excessive energy penalty, considering that the main objective of this stage is to remove compounds that are undesirable from the point of view of energy production, while maintaining enough volatile matter in the solids to produce combustible liquid and gaseous fractions in the subsequent stages of the process.

As temperature increases, the decreasing energy content of torrefied sewage sludge should parallel some changes in the compositions of liquid and gaseous fractions. For instance, the water content of the liquid fraction was determined by means of Karl-Fischer titration. The results are shown in Table 3. For the experiments carried out at 250ºC, it can be considered that water is the only liquid product.

Table 3. Water content of the liquid fractions from fixed bed torrefaction experiments.

Temperature (ºC)	Weight % of H_2O
250	100.0
300	93.4 ± 0.0
350	78.5 ± 2.9

As sewage sludge decomposition is taken to greater extents, the formation of organic liquid products is evidenced by a decrease in the water content. This decrease is still very low at 300ºC, but reaches 21.5% of the condensed liquid at 350ºC. Obviously, the release of organic compounds in the torrefaction stage is not desirable from an energy efficiency point of view.

From the combination of these data and those presented in Table 2, at 250ºC 15.3% of sludge is converted to water. This percentage increases to 18.6% and 20.8% at 300 and 350ºC, respectively. In any case, these results show that a very important fraction of the total amount of water generated during pyrolysis is formed at these low temperatures, as shown in previous studies[10,23,24]. Finally, at 300ºC, 1.3% of the original sludge weight is converted into organic liquids, whereas this percentage grows to 5.7% at 350ºC.

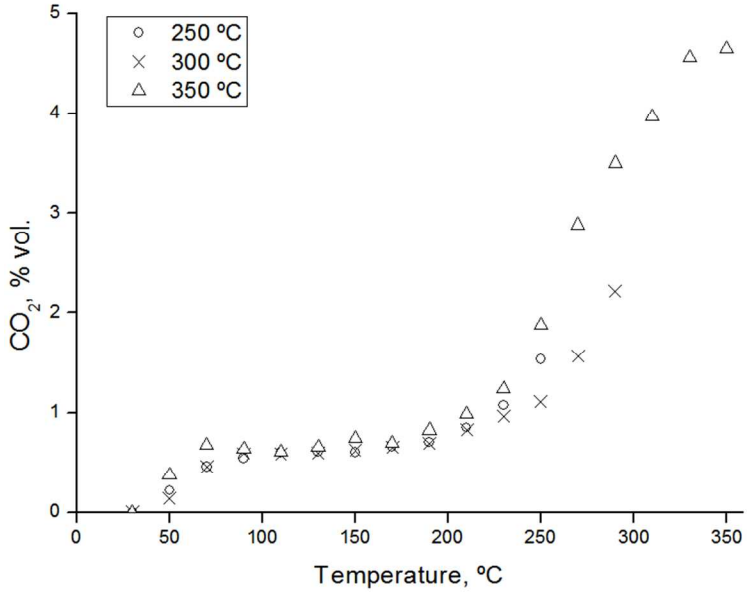

Figure 3. CO_2 content of product gases in the fixed bed torrefaction experiments (percentages including nitrogen used as inert gas.)

CO_2 is the only gaseous product significantly detected (only traces of other gases were found in the experiments carried out at 250 and 300ºC). Figure 3 shows that this compound evolves mainly beyond 200ºC. In contrast, at 350ºC compounds such as H_2, CH_4, C_2H_4, C_2H_6 and H_2S were clearly detected, as can be seen in Figure 4. Again, the presence of hydrocarbons demonstrates that a working temperature of 350ºC is not advisable because there is less carbon and hydrogen available for bio-oil and/or combustible gases formation in the main stage of pyrolysis.

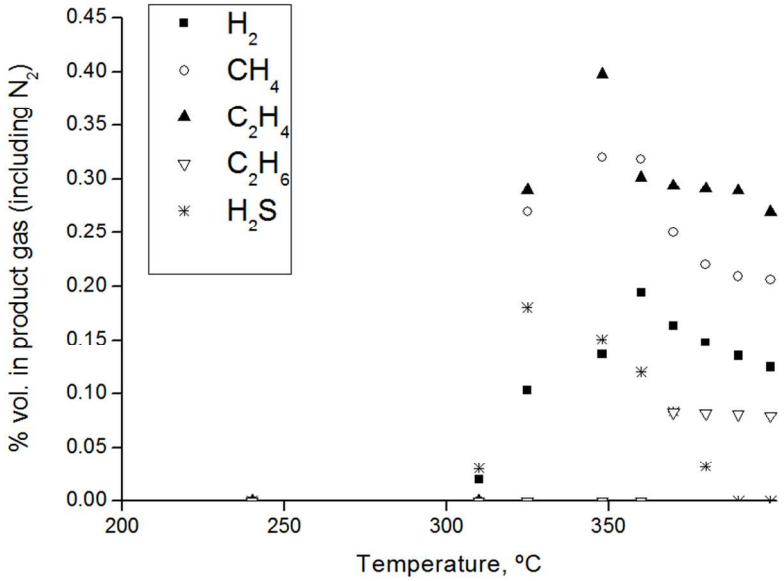

Figure 4. Other gases detected in the torrefaction experiment at 350ºC. Values beyond 350ºC correspond to the hold time of 30 minutes after reaching target temperature.

In view of the torrefaction results and having discarded 350ºC, the most suitable torrefaction temperature among the three tested seems to be 300ºC. In these conditions, a great amount of water is generated (18.6% of the initial mass of sewage sludge) with almost no other liquid formation. Moreover, the product gases are almost exclusively carbon dioxide. Both effects should be beneficial from the point of view of the energy content of gaseous and liquid products from pyrolysis.

3.1.2. FLUIDIZED BED TORREFACTION EXPERIMENTS

The previous Section explored the potential advantages of torrefaction as a previous stage for fast pyrolysis of sewage sludge or other biomass materials. In that case, torrefaction was done by applying a slow heating rate in a fixed bed reactor; nevertheless, it is also interesting to determine if high heating rates in other types of reactor (i.e. a fluidized bed) can also produce similar results. In addition, this was also convenient because of the size limitations of our experimental systems; using the small fixed bed reactor for making torrefied sludge for its use in fluidized bed pyrolysis was found to be impractical due to the extremely high number of experiments required to achieve a significant amount of material to carry out the rest of the experiments.

Thus, fluidized bed torrefaction of sewage sludge was carried out at the optimum temperature previously determined (300ºC). The product yields from these experiments were 82.8 % wt. solids, 12.2% liquid and 5.1% gases.

Results are not the same as those from fixed bed torrefaction. For instance, solid yield is higher (and close to that produced at 250ºC in fixed bed experiments), whereas gas and liquid yields are lower (especially the latter). This is a consequence of the different designs and operating principles in these two types of reactors. In fixed bed experiments, solid samples were maintained for an additional hold time of 30 minutes after reaching 300ºC. In the fluidized bed reactor, the residence time for solids inside the bed is estimated to be around 6 minutes. Moreover, heating rates are much higher because heat transfer is greatly enhanced in the case of fluidized bed torrefaction.

The water content of the liquid fraction was also determined and found to be 93.5%, which is almost identical to that determined for fixed bed experiments at the same temperature. Nevertheless, and because of the lower liquid yield, the total amount of water resulting from this stage is lower, 11.4% of the original sewage sludge mass.

Gas chromatograms showed a stable composition throughout the experiment time. Unlike fixed bed gases, CO_2 was not the only compound present in the stream. On average, H_2S represented 4.2 vol. % of gases on a N_2 free-basis. Traces of hydrocarbons (CH_4, C_2H_4 and C_2H_6) were also detected. These results suggest that an increase of temperature at this stage is not advisable because of the potential formation of hydrocarbons. On the other hand, the evolution of H_2S might represent a good opportunity for sulfur removal prior to the pyrolysis stage.

The ultimate analysis of torrefied sewage sludge from fluidized bed experiments is presented in Table 4. These data can be compared to the original sewage sludge composition shown in Table 1 to show that more than half of the oxygen from sludge is lost after torrefaction (55.6%), mostly in the form of carbon dioxide and water, while the rest of the elements show lower weight losses. The observed weight loss trends seem to be in accordance with the previous observations about gas and liquid compositions. A remarkable difference is that the heating value of the torrefied solid increases compared to the raw sewage sludge.

Table 4. Ultimate analysis, ash content and heating value of solids from fluidized bed torrefaction, and percentage of weight loss of each element.

Ultimate analysis (Carlo Erba 1108)	% weight	% weight loss*
C	28.6	12.6
H	3.7	28.2
N	4.7	3.5
S	0.6	17.2
O (by diff.)	11.6	55.6
Ash content	50.9	-
Heating Value		
HHV(MJ/kg)	13.2	

*relative to the original sewage sludge composition (see Table 1).

The importance of oxygen reduction during torrefaction is well illustrated in Van Krevelen's diagram, which represents the hydrogen to carbon ratio in function of the oxygen carbon ratio[25]. A similar diagram for the torrefaction process (using sewage sludge as-received) is depicted in Figure 5.

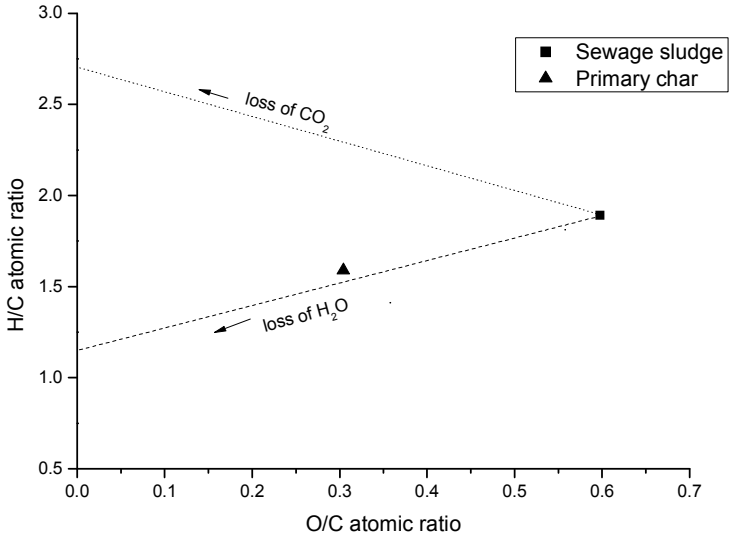

Figure 5. Van Krevelen's diagram for sewage sludge torrefaction.

As seen on Figure 5, the O/C ratio of torrefied solids decreases by more than 40% compared to the initial O/C ratio for sludge, whereas the H/C atomic ratio is only slightly reduced during the process. Figure 5 also includes the theoretical lines of H_2O and CO_2 loss from the original sewage sludge, showing that the main effect of torrefaction is the formation of water and, to a lesser extent, of CO_2.

As a conclusion, the fluidized bed torrefaction stage seems a suitable pretreatment prior to pyrolysis, because it increases the energy density of the solid and generates the desired activating agents required for the adsorbent production stage.

3.2. PYROLYSIS STAGE

The main objective of a fast pyrolysis stage is the attainment of a significant amount of liquid fraction or bio-oil; thus, experiments were carried out in the fluidized bed reactor[26]. Additionally, a combustible

gas mixture and a pyrolysis char would be obtained. Temperature is the main operational parameter that influences the yields of pyrolysis products. Accordingly to our previous results using a similar sewage sludge[8], the selected pyrolysis temperature was 550ºC.

3.2.1. PRODUCT YIELDS

The product yields from this stage are 69.1 % wt. solids, 23.3 % wt. liquids and 7.6 % wt. gases (on a torrefied sludge basis). Due to the high ash content of sewage sludge, the main product is pyrolysis char, whereas about one quarter of the torrefied sludge is converted into the liquid fraction. Previous works with sewage sludge from the same wastewater treatment plant, in the same experimental facility and at the same temperature[27] provide the best reference for comparing these results with those from a single stage pyrolysis, as shown in Figure 6.

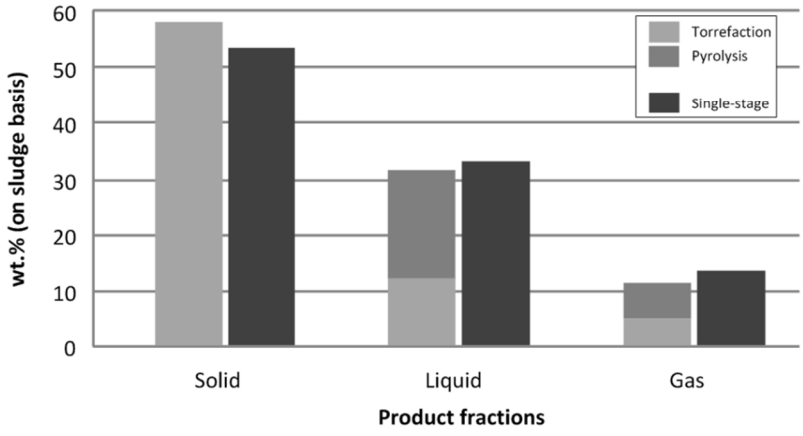

Figure 6. Product yields from this work and from single-stage pyrolysis.

Product yields from a single-stage pyrolysis and from the combination of torrefaction and pyrolysis are quite similar. For instance, the total amount of liquids from both stages is 31.5% in this work, and 32.8% from single-stage pyrolysis. Somewhat higher differences are found in the solid fraction (57.2% and 53.3%, respectively).

3.2.2. LIQUID FRACTION

The liquid fraction from fluidized bed pyrolysis of sewage sludge is usually divided in two phases, organic and aqueous[28–31]. However, centrifugation of the liquid fraction from this stage produced three well-defined phases, as previously seen by Fonts et al[27,32]: top or light organic phase, middle or viscous organic phase and bottom or aqueous phase . Some of the characteristics of each of these phases are shown in Table 5. As a major consequence of the removal of water in the torrefaction process, there is a great reduction in the water content and yield of the aqueous phase, whereas the overall water yield for single-stage pyrolysis is similar to that of torrefaction + pyrolysis (15.7% and 17.9% respectively, on a sewage sludge basis). In this sense, applying a torrefaction stage produces a higher quality bio-oil, because reduced water content increases stability and overall heating value of this product[33].

Table 5. Product yields from the pyrolysis stage and comparison with data from single-stage pyrolysis taken from previous work[8] .

	Torrefaction + pyrolysis			Single-stage pyrolysis		
Water yield (wt. %)	17.9[a] ± 0.8			15.7 ± 0.6		
Phase	Light	Viscous	Aqueous	Light	Viscous	Aqueous
Yield (wt. %)	1.7 ± 0.1	8.3 ± 0.6	9.3 ± 0.4	2.2 ± 0.2	9.4 ± 0.5	20.3 ± 0.5
Water content (wt. %)	0.0	5.0 ± 0.4	66.1 ± 0.9	0.0	6.4 ± 0.7	73.8 ± 0.6
Higher heating value (MJ/kg)	42.8 ± 0.3	32.8 ± 0.9	6.76 ± 0.3	43.1 ± 0.1	31.7 ± 1.9	5.18 ± 0.3

[a] Includes water from torrefaction and pyrolysis

The product yields, water content and heating value of the light and viscous liquid phases were less affected by the previous torrefaction stage, as can be seen in Table 5. Densities from the three identified phases are 0.90, 1.05 and 1.08 kg/dm^3 (light, viscous and aqueous, respectively). Table 6 presents elemental analyses for each phase (on a water free basis) and compares them with values from single-stage pyrolysis. Either applying a previous torrefaction stage or carrying out a single pyrolysis stage, very similar chemical compositions of each one of these phases are obtained. Thus, in terms of liquid

yield, one significant advantage of a torrefaction stage is a reduction on water content, without negative effects on the composition of the organic liquid fraction. In contrast, if water removal steps are required after single-step pyrolysis, a significant fraction of organic compounds might be lost from the liquid[34].

Table 6. Elemental analysis of phases from the pyrolysis oil on a water free basis, and comparison with single-stage pyrolysis.

(Wt. %)	Torrefaction + Pyrolysis			Single-stage pyrolysis		
Phase	Light	Viscous	Aqueous	Light	Viscous	Aqueous
C	85.6	73.4	43.4	85.9	74.5	43.0
H	11.5	7.7	4.0	11.8	8.8	8.6
N	2.2	11.9	26.0	1.8	10.1	25.1
S	0.4	0.7	1.2	0.2	1.3	1.4
O	0.3	6.3	25.5	0.3	5.3	22.0

Finally, the special characteristics of sewage sludge (very high sulfur and nitrogen contents) are reflected in the liquid products. Comparing these values with those from Table 1, it seems that nitrogen tends to accumulate in the liquid product, unlike sulfur, which appears in small amounts in the liquid phases.

The low content of oxygenated compounds in the light and viscous phases is remarkable, and could indicate good characteristics for storage and use as a fuel. On the other hand, the presence of high N and S contents in the viscous and aqueous phases could make their use as a fuel unadvisable without further treatments[32]. However, the extremely high N content of the aqueous phase, together with its presumably low heating value, could make it a potential fertilizer[35].

3.2.3. GASEOUS FRACTION

The average gas composition obtained during fluidized bed pyrolysis of torrefied sludge (in a N_2-free basis) is shown in Table 7. The gas heating value was calculated from these results and is also presented

in Table 7. As can be seen, the main compound is carbon dioxide even after the torrefaction stage, and light hydrocarbons are found in high concentrations. The H_2S content is also high, which could be its main drawback for producing energy by means of combustion. The overall heating value of the pyrolysis gas is higher than 13.3 MJ/m^3(STP), which is the value obtained at 550 ºC from single-stage pyrolysis of the same sludge[8]. This can be attributed to the removal of carbon dioxide during torrefaction.

Table 7. Composition and heating value of pyrolysis gas

Compound	Vol. %
H_2	14.9
CO	12.8
CO_2	45.2
CH_4	14.6
C_2H_4	6.5
C_2H_6	3.6
H_2S	2.4
Heating Value	
MJ/m^3(STP)	14.6

3.2.4. SOLID FRACTION

The pyrolysis char obtained from this stage has the following elemental composition by weight: 16.12% C, 0.93% H, 2.10% N, 0.35% S and 6.74% O (by difference), with 73.76% ash. Figure 7 shows the compositional changes of solids through torrefaction and pyrolysis on a sludge weight basis. The relative weight losses of C and H are much higher during the pyrolysis stage than in torrefaction, while the opposite applies to O. As seen before, these trends are beneficial for obtaining liquid and gaseous

products with higher energy contents. However, N release is higher during pyrolysis, and S loss is almost constant, which is detrimental for the same purpose.

Finally, the pyrolysis char had a BET surface area of 29.4 m^2/g and a heating value of 5.75 MJ/kg (28.8% of the heating value from raw sewage sludge).

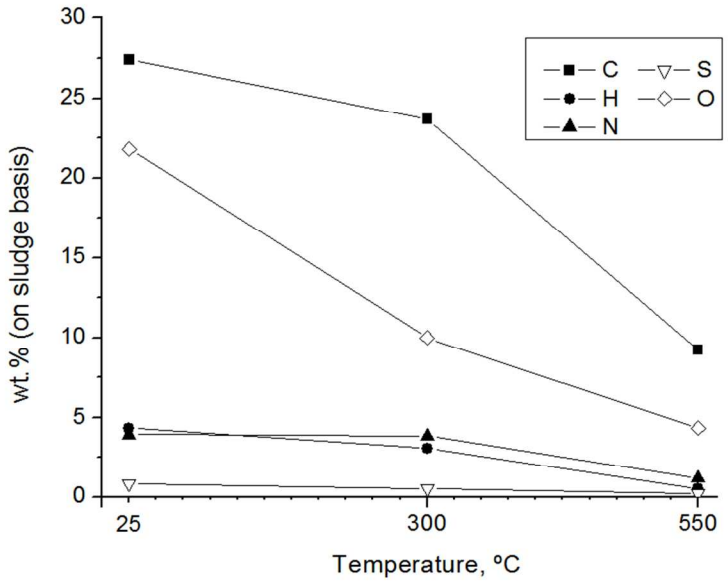

Figure 7. Compositional changes of solids through torrefaction and pyrolysis.

3.3. PYROLYSIS CHAR ACTIVATION STAGE

As explained before, the pyrolysis char activation experiments were carried out in two steps: the first step (heating or pyrolysis) was performed in a N_2 atmosphere to achieve the desired final temperatures, and the second was the isothermal activation step which used the same amount of CO_2 and H_2O evolved in the torrefaction step.

3.3.1. HEATING STEP

Product yields and BET surface areas of solids after the heating step are summarized in Table 8. The solid weight loss is low (below 15% at both temperatures tested), and increasing the temperature from 750 to 850ºC only produces an increase in the gas yield, which suggests that there is no liquid formation beyond 750ºC. The small liquid fraction (that could also be added to the subsequent activation step) was

watery-like, and its yield was too small to be analyzed. The BET surface area increased with temperature (at 850ºC it is almost double than that of pyrolysis char), similar to previous results[20].

Table 8. Product yields and BET surface areas of solids from the heating step prior to activation.

T(ºC)	Yield, wt.%			BET surface area, m^2/g
	Solid	Liquid	Gas	
750	90.0 ± 0.2	2.7 ± 0.5	7.3 ± 0.6	42.6
850	86.0 ± 0.1	2.8 ± 0.3	11.2 ± 1.3	56.6

The evolution of gases during this step is similar to that described by Ábrego et al.[20], and can be seen in Figure 8. The average composition of gases is (on a N_2-free basis): 37.4% H_2, 37.0% CO, 3.1% CH_4 and 22.5% CO_2, with a heating value of 9.8 MJ/m^3(STP). Interestingly, only trace amounts of H_2S were detected during the runs.

Figure 8. Evolution of gases from the heating step up to 850 ºC.

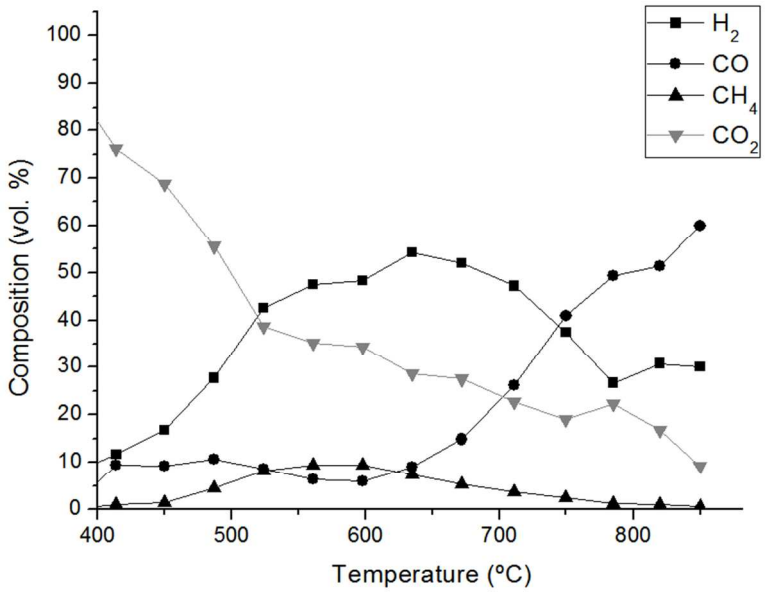

3.3.2. ACTIVATION STEP

The activation step produced additional solid weight losses of 1.5 and 2.0% at 750 and 850ºC, respectively (on a pyrolysis char basis). A small amount of liquid product was detected in the condensation vessel, although it could not been quantified. BET surface areas increased after activation to 52.7 m^2/g (750ºC) and 74.5 m^2/g (850ºC). Figure 9 depicts the adsorption isotherms (N_2, 77K) of the solid materials involved in this stage. These results can be used to identify changes in the pore structure during the heating and activation steps.

Figure 9. Adsorption isotherms from the activation stage.

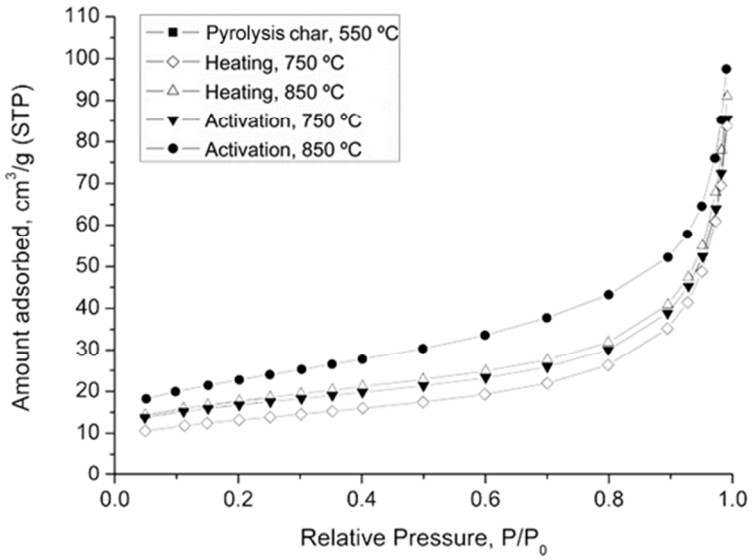

The isotherm shapes suggest predominant mesoporosity[36], although microporosity seems to develop to some extent with increasing heating and activation temperatures. Both heating without activation at 850ºC and activation at 750ºC lead to very similar pore structures, whereas activation at 850ºC produces the highest micropore development, as revealed by the increasing adsorbed amounts at low relative pressures. This treatment also seems to produce a broader mesopore distribution, as suggested by the increasing slope of the curve at intermediate relative pressures. Both effects on porosity may be attributed to the use of water vapor and CO_2 as simultaneous physical activation agents. Works carried out with biomass materials at similar temperatures[37,38] concluded that carbon dioxide produces the

development of narrow microporosity and further pore widening, while steam activation produces meso- and macroporosity development with a wider pore distribution as a result. These conclusions follow the previously observed trends.

Although the BET surface areas of the activated chars seem low, they have been successfully tested in a wide range of adsorption applications, probably due to their distinctive combination of porosity and favorable surface chemistry[11].

Table 9 shows the elemental composition of the product char and a comparison with the pyrolysis char. The decreasing carbon content of the samples appears to be closely related to the previously explained increase in microporosity, as revealed by the adsorption isotherms. A significant loss of hydrogen and nitrogen is found, especially for activation at 850 ºC. Unfortunately, and due to the lack of specific analysis equipment, nitrogen compounds could not be detected in the gaseous stream. Finally, the sulfur enrichment of the samples suggest persistence of this element in the solid matrix, as confirmed by previous works[20] and the negligible H_2S release during the heating step.

Table 9. Elemental analysis of the solids from the activation stage.

	Wt. %			
	C	H	N	S
Pyrolysis char (550ºC)	16.1	0.9	2.1	0.4
Heating (750ºC)	14.8	0.4	1.4	0.4
Heating (850ºC)	14.1	0.3	0.9	0.5
Activation (750ºC)	14.0	0.3	1.1	0.5
Activation (850ºC)	11.6	0.2	0.6	0.5

The evolution of gases during activation at 850ºC (Figure 10) gives additional insight about how the physical activation process occurs. The main product gases were H_2, CO and CO_2, and traces of CH_4 were also detected. CO decreases as activation advances. H_2 shows a slower decrease, and CO_2 reaches

its minimum concentration in the first quarter of the experiment. These behaviors may indicate that CO_2 plays an important role at the beginning of the activation process, when most of this gas is consumed, but its effectiveness is reduced as pore enlargement occurs. The more stable evolution of H_2 could suggest that H_2O activation proceeds throughout the experiment.

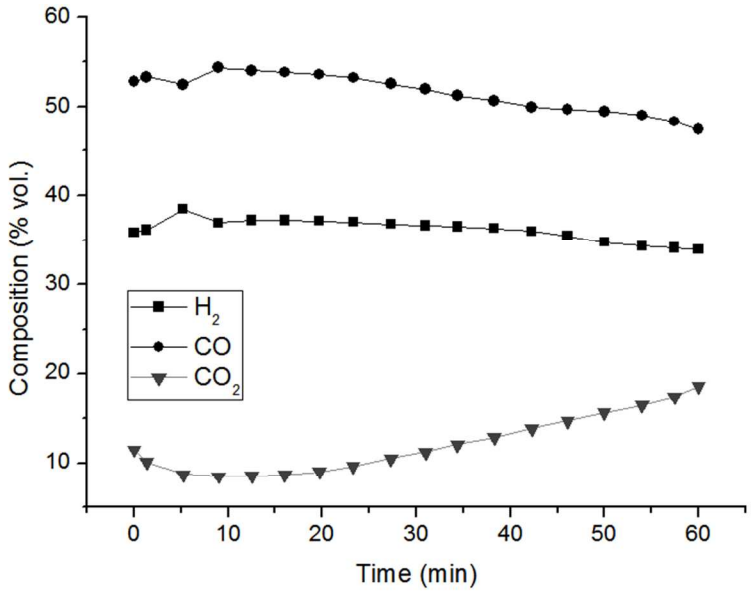

Figure 10. Evolution of gases during activation at 850 ºC.

Finally, the average heating value of the gas mixture was found to be 10.5 MJ/m^3(STP).

4. MASS AND ENERGY OUTPUTS FOR THE PROCESS

4.1. MASS BALANCE

To put all these results in perspective, Figure 11 shows a Sankey diagram for the mass balance of the overall process. In this diagram, the width of each arrow represents its relative importance expressed in weight percent. As can be seen, the major product on a mass basis is the final (activated) char, representing 48.2 % wt. of the total sludge mass. The total combustible gases are estimated to sum up to 30.6 % wt. of the original sludge mass, and the liquid product obtained was 19.3%. It was assumed that all the gaseous streams are combined for their final use (for energy purposes) in a subsequent stage; thus, a sole gas stream is represented in the diagram (N_2 for creating non-oxidizing atmosphere and

fluidization is not included). However, this gas stream contains a significant amount of H_2S, which would be a drawback for energy purposes, and some unreacted water from the activation stage.

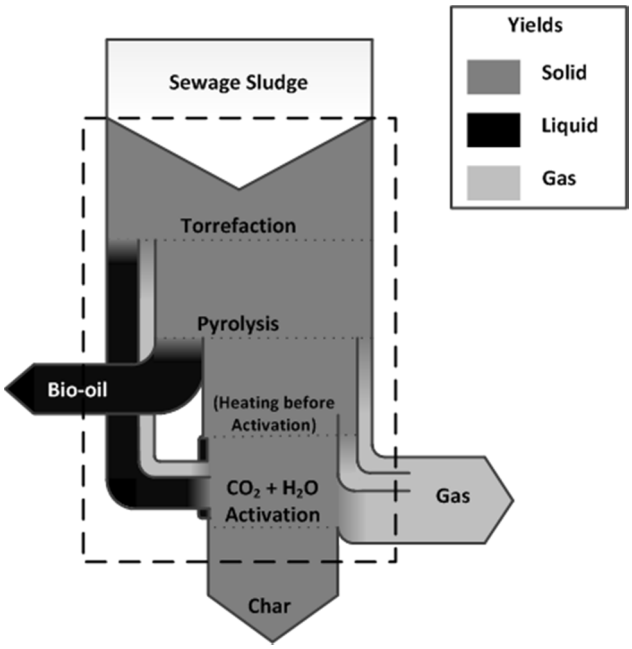

Figure 11. Sankey diagram representing the mass outputs from the process.

4.2. ENERGY BALANCE

Considering the control volume shown in Figure 12, a preliminary energy balance was carried out for the process. If no heat losses are considered, the following equation should be satisfied:

$$\Delta H_{in} + Q = \Delta H_{out} \quad \text{(Eq. 1)},$$

with ΔH_{in} and ΔH_{out} representing the enthalpy of the streams entering and exiting the control volume, respectively, and Q the heat (per kg of sewage sludge) needed for the process.

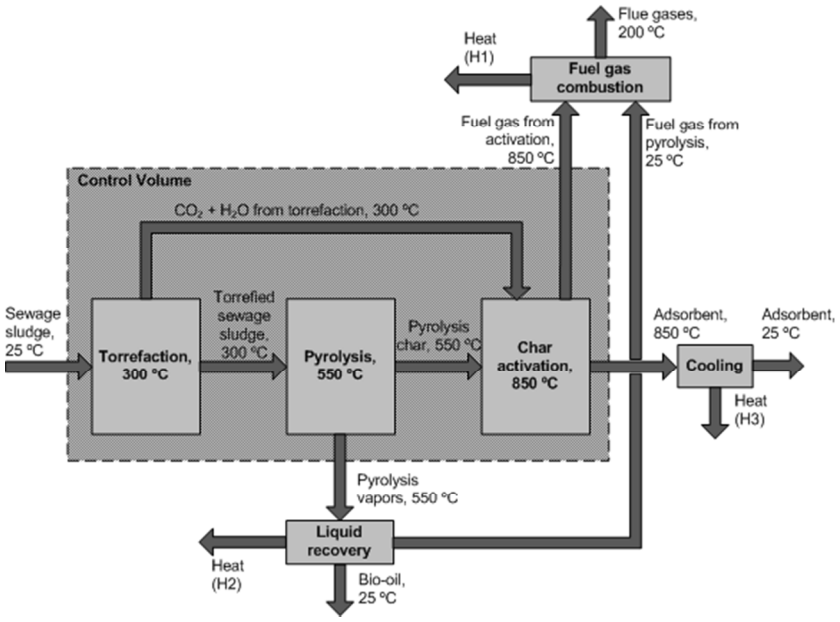

Figure 12. Energy balance of the process.

The standard enthalpies of formation of the liquid and solid products from the process (bio-oil and adsorbent), as well as the sewage sludge, can be calculated from their higher heating values and the enthalpies of their combustion products, according to Equation 2:

$$\Delta H_{f^\circ,\, apparent} = HHV - \Delta H_{f^\circ,\, combustion\ products} \qquad \text{(Eq. 2)}$$

To calculate the enthalpy of each stream at its temperature, the term $m \cdot C_p \cdot \Delta T$ and the enthalpy of phase change (if any) should be added to the standard enthalpy of formation of each species. The data used for enthalpy calculations can be found in the 'Supplementary Material' Section of this article. Inert gases such as nitrogen for fluidization were not included in the energy balance.

In Figure 12, several heat streams can be obtained from combusting the fuel gases from the process (H1) or cooling the hot products (H2 and H3). It was assumed that only H1 can be practically recovered in order to deliver the energy needed for the process.

Results from the energy balance are summarized in Table 10. The total energy input needed to drive the process is 1019 kJ/kg of dry sewage sludge (around 10% of the initial energy content of sewage

sludge). The combustion of the fuel gases with stoichiometric air (stream H1 from Figure 12) would release 2458 kJ per kg of sewage sludge. Even considering the use of excess air, relatively high heat losses, low heat exchange efficiencies and the use of inert gases and bed materials for fluidization (not considered in these calculations), H1 can probably provide the required energy. Nevertheless, the high content of H_2S in the product gas would require a cleaning step before combustion.

Table 10. Results from the energy balance calculations.

	kJ/kg SS
Heat needed for the process, $Q = \Delta H_{out} - \Delta H_{in}$ (kJ/kg SS)	**1019**
Heat from each Product Stream[a] (according to Figure 12)	
H1 (Combustion of fuel gases, cooling of flue gases to 200 ºC)	-2458
H2 (Liquid condensing and cooling to 25 ºC)	-471
H3 (Activated char cooling to 25 ºC)	-456
$\Delta H_{out} - \Delta H_{in}$ for each individual step of the process	
Heat of torrefaction	870
Heat of pyrolysis	-685
Heat of activation	834

[a]Outside the volume control.

Table 10 also shows that the torrefaction process requires an energy input to be carried out (870 kJ/kg SS), whereas the pyrolysis stage releases 685 kJ/kg SS. Combining torrefaction and pyrolysis, the overall energy requirement is 185 kJ/kg SS. Van de Welden et al.[39] reported a higher value of 385 kJ/kg for TGA experiments using sewage sludge. The exothermicity of the pyrolysis step can be related to char forming reactions[40,41].

5. CONCLUSIONS

- Suitable temperatures for each stage of the proposed process have been determined: 300ºC for torrefaction, 550ºC for pyrolysis and 850ºC for char activation. The solid fraction, according

to its characteristics, can be used as an adsorbent. The activation stage increases its surface area and microporosity, and generates an additional fuel gas stream.

- The overall gaseous fraction (combining gaseous outputs from pyrolysis and activation) can be used as a fuel; nevertheless, its relatively high H_2S content suggests the need of a removal step.
- The main consequence of the previous torrefaction process is the reduced water content in the pyrolysis liquid (when compared to single-step pyrolysis). The liquid fraction from pyrolysis can be easily separated in three fractions via centrifugation. The upper and middle phases seem suitable for fuel use; however, nitrogen tends to accumulate in the bottom phase, which together with its high water content makes it unsuitable for energy purposes, but might encourage its use as fertilizer with further conditioning steps.
- A preliminary energy balance of the process shows that the total energy input needed to drive the process is around 10% of the total energy content of sewage sludge. Fuel gas combustion could lead to autothermal operation.

6. ACKNOWLEDGMENTS

The authors thank the funds provided by the Spanish Ministry of Economy and Competitiveness through project CTQ2010-20137. N. Gil-Lalaguna also expresses her gratitude to the Ministry for the doctoral grant received. The authors also thank Lindsey Deignan from UNCW, USA for her valuable advice.

7. SUPPORTING INFORMATION AVAILABLE

A MS Excel® file includes the detailed energy balance calculations. This information is available free of charge via the Internet at http://pubs.acs.org/.

8. REFERENCES

(1) Bridle, T. R.; Molinari, L.; Skrypski-Mantele, S.; Ye, P. D.; Mills, J. *Water Sci. Technol.* **2000**, *41*, 31–36.

(2) Skrypski-Mantele, S.; Bridle, T. R.; Freeman, P.; Luceks, A.; Ye, P. D. *Water Sci. Technol.* **2000**, *41*, 45–52.

(3) Yoshida, T.; Antal Jr, M. J. *Energ. Fuel.* **2009**, *23*, 5454–5459.

(4) Fonts, I.; Gea, G.; Azuara, M.; Ábrego, J.; Arauzo, J. *Renew. Sust. Energ. Rev.* **2012**, *16*, 2781–2805.

(5) Bridgwater, A. V.; Peacocke, G. V. C. *Renew. Sust. Energ. Rev.* **2000**, *4*, 1–73.

(6) Kim, Y.; Parker, W. *Bioresource Technol.* **2008**, *99*, 1409–1416.

(7) Shen, L.; Zhang, D.-K. *Fuel* **2003**, *82*, 465–472.

(8) Fonts, I.; Juan, A.; Gea, G.; Murillo, M. B.; Sánchez, J. L. *Ind. Eng. Chem. Res.* **2008**, *47*, 5376–5385.

(9) Rocha, J. D.; Luengo, C. A.; Snape, C. E. *Org. Geochem.* **1999**, *30*, 1527–1534.

(10) Westerhof, R. J. M.; Kuipers, N. J. M.; Kersten, S. R. A.; van Swaaij, W. P. M. *Ind. Eng. Chem. Res.* **2007**, *46*, 9238–9247.

(11) Smith, K. M.; Fowler, G. D.; Pullket, S.; Graham, N. J. D. *Water Res.* **2009**, *43*, 2569–2594.

(12) van der Stelt, M. J. C.; Gerhauser, H.; Kiel, J. H. A.; Ptasinski, K. J. K. J. K. J. K. J. *Biomass Bioenerg.* **2011**, *35*, 1–15.

(13) Prins, M. J.; Ptasinski, K. J.; Janssen, F. *Energy* **2006**, *31*, 3458–3470.

(14) Couhert, C.; Salvador, S.; Commandré, J.-M. *Fuel* **2009**, *88*, 2286–2290.

(15) Mani, S. In *AIChE Annual Meeting 2009*; Nashville, TN, USA, 2009.

(16) Ábrego, J.; Casado, B.; García, G.; Sánchez, J. L.; Gonzalo, A. In *17th European Biomass Conference & Exhibition*; Hamburg, 2009; pp. 1140–1142.

(17) Meng, J.; Park, J.; Tilotta, D.; Park, S. *Bioresource Technol.* **2012**, *111*, 439–446.

(18) Prins, M. J.; Ptasinski, K. J.; Janssen, F. *J. Anal. Appl. Pyrol.* **2006**, *77*, 35–40.

(19) Bergman, P. C. A.; Boersma, A. R.; Zwart, R. W. R.; Kiel, J. H. A. *Torrefaction for biomass co-firing in existing coal-fired power stations, Report ECN-C-05-013*; Petten, The Netherlands, 2005.

(20) Ábrego, J.; Arauzo, J.; Sánchez, J. L.; Gonzalo, A.; Cordero, T.; Rodríguez-Mirasol, J. *Ind. Eng. Chem. Res.* **2009**, *48*, 3211–3221.

(21) García, G.; Cascarosa, E.; Ábrego, J.; Gonzalo, A.; Sánchez, J. L. *Chem. Eng. J.* **2011**, *174*, 644–651.

(22) Manyà, J. J.; Sánchez, J. L.; Ábrego, J.; Gonzalo, A.; Arauzo, J. *Fuel* **2006**, *85*, 2027–2033.

(23) García-Pérez, M.; Wang, X. S.; Shen, J.; Rhodes, M. J.; Tian, F.; Lee, W.-J.; Wu, H.; Li, C. Z. *Ind. Eng. Chem. Res.* **2008**, *47*, 1846–1854.

(24) Westerhof, R. J. M.; Brilman, D. W. F. (Wim); van Swaaij, W. P. M.; Kersten, S. R. A. *Ind. Eng. Chem. Res.* **2010**, *49*, 1160–1168.

(25) van Krevelen, D. W. *Fuel* **1950**, *29*, 269–284.

(26) Bridgwater, A. V. V.; Meier, D.; Radlein, D. *J. Anal. Appl. Pyrol.* **1999**, *51*, 3–22.

(27) Fonts, I.; Gil, N.; Azuara, M.; Lázaro, L.; Murillo, M. B. In *17th European Biomass Conference & Exhibition*; ETA- Florence Renewable Energies: Hamburg, 2009; 1161–1165.

(28) Bridle, T. R.; Pritchard, D. *Water Sci. Technol.* **2004**, *50*, 169–175.

(29) Inguanzo, M.; Domínguez, A.; Menéndez, J. A.; Blanco, C. G.; Pis, J. J. *J. Anal. Appl. Pyrol.* **2002**, *63*, 209–222.

(30) Kaminsky, W.; Kummer, A. B. *J. Anal. Appl. Pyrol.* **1989**, *16*, 27–35.

(31) Pokorna, E.; Postelmans, N.; Jenicek, P.; Schreurs, S.; Carleer, R.; Yperman, J. *Fuel* **2009**, *88*, 1344–1350.

(32) Fonts, I.; Kuoppala, E. T.; Oasmaa, A. *Energ. Fuel.* **2009**, *23*, 4121–4128.

(33) Bridgwater, A. V. *Biomass. Bioenerg.* **2011**, *38*, 68–94.

(34) Gil-Lalaguna, N.; Fonts, I.; Gea, G.; Murillo, M. B.; Lázaro, L. *Energ. Fuel.* **2010**, *24*, 6555–6564.

(35) Azuara, M.; Ábrego, J.; Fonts, I.; Gea, G.; Murillo, M. B. In *Proceedings of the 18th European Biomass Conference and Exhibition*; Lyon, France, 2010; pp. 993–996.

(36) Bagreev, A.; Bandosz, T. J.; Locke, D. C. *Carbon* **2001**, *39*, 1971–1979.

(37) Rodríguez-Reinoso, F.; Molina-Sabio, M.; Gonzalez, M. T. *Carbon* **1995**, *33*, 15–23.

(38) Cordero, T.; Márquez-Montesinos, F.; Rodríguez-Mirasol, J.; Rodríguez, J. J. *Fuel* **2002**, *81*, 423–429.

(39) Van de Velden, M.; Baeyens, J.; Brems, A.; Janssens, B.; Dewil, R. *Renew. Energ.* **2010**, *35*, 232–242.

(40) Milosavljevic, I.; Oja, V.; Suuberg, E. M. *Ind. Eng. Chem. Res.* **1996**, *35*, 653–662.

(41) Mok, W. S.-L.; Antal, M. J. *Thermochim. Acta* **1983**, *68*, 165–186.